Dental Materials Journal 2023; 42(3): 319–326

Bone augmentation with a prototype coral exoskeleton-derived bone replacement material applied to experimental one-wall infrabony defects created in alveolar bone

Hayato IKEDA[1], Tomoharu OKAMURA[2], Tetsunari NISHIKAWA[3], Nobuhiro KOBAYASHI[4], Yoshiya HASHIMOTO[5], Kazuya TOMINAGA[2] and Tomio ISEKI[1]

[1] *Department of Oral and Maxillofacial Surgery I, School of Dentistry, Osaka Dental University, 8-1 Kuzuhahanazono-cho, Hirakata, Osaka 573-1121, Japan*
[2] *Department of Oral Pathology, School of Dentistry, Osaka Dental University, 8-1 Kuzuhahanazono-cho, Hirakata, Osaka 573-1121, Japan*
[3] *Center of Innovation in Dental Education, School of Dentistry, Osaka Dental University, 8-1 Kuzuhahanazono-cho, Hirakata, Osaka 573-1121, Japan*
[4] *Department of Oral Implantology, School of Dentistry, Osaka Dental University, 8-1 Kuzuhahanazono-cho, Hirakata, Osaka 573-1121, Japan*
[5] *Department of Biomaterials, School of Dentistry, Osaka Dental University, 8-1 Kuzuhahanazono-cho, Hirakata, Osaka 573-1121, Japan*
Corresponding author, Tomoharu OKAMURA; E-mail: okamu-t@cc.osaka-dent.ac.jp

Bone regeneration requires cells, growth factors, and scaffolds that should have biocompatibility, porosity, and physical strength. Therefore, coral granules (CG) with diameters of 600–1,000 μm were prepared as a potential graft material from cultured edaphic thermostable corals. X-ray and electron microscopy characterization revealed that CGs were porous and permeable with lumen diameters of approximately 200 μm. Human periodontal ligament fibroblasts showed significantly increased mitochondrial activity in culture seven days after adding CG. After CG filling into an experimentally created one-wall infrabony defect in a beagle dog jawbone, the defect almost completely disappeared within approximately 8 weeks, and bone tissue growth was observed in the replacement area. This could indicate extremely rapid healing of a bone defect previously considered incapable of self-healing. Based on stable supply of cultured coral (*Montipora digitata*), CG is potentially an ideal replacement material for alveolar and jawbone defects.

Keywords: Coral, One-wall infrabony defects, Bone regeneration, Periodontal ligament

INTRODUCTION

Cells, scaffolds, and growth factors are necessary elements for jawbone and alveolar bone regeneration[1,2]. Improvements in bioabsorbability, which could shorten treatment duration, will be an important factor for developing scaffold materials in the future. The jawbone and alveolar bone, which perform oral functions such as mastication, occlusion, swallowing, and pronunciation are subject to physical forces. Therefore, scaffold materials used for alveolar bone regeneration must be strong[3-5]. Although physical strength is required, scaffold materials should also possess biocompatibility and absorbability[4,6]. The bioabsorbability factor requires porous scaffolds. However, increasing porosity tends to reduce physical strength. Therefore, scaffold material that is porous and bioabsorbable with physical strength is ideal for jawbone regeneration. Nishikawa *et al*.[7] previously reported that the coral exoskeleton had physical strength that approximated that of rat femur with excellent bioabsorbability. This physical strength contributed to maintaining the bone replacement material in place and enhancing its bioabsorbability.

Therefore, we focused on coral exoskeletons, which have ideal scaffold material conditions and have been clinically utilized in the United States and Europe. The coral exoskeleton is a hard tissue composed of calcium carbonate and, unlike the mammalian skeleton, contains no organic matter. It has porous structure, with pore diameters of approximately several hundred micrometers, depending on coral species[3]. It has good biocompatibility and is completely absorbable[4].

The corals that have been used for synthesizing medical devices in Europe and the United States are of the Scleractinia lineage[8]. Although *Goniopora* species are porous, they have capsular walls that can hinder cell invasion[9]. Therefore, we focused on the characteristics of coral exoskeletons that lack capsular walls and have high porosity. In addition, we examined coral species whose coral exoskeleton pore size was suitable for jawbone and alveolar bone regeneration. Furthermore, considering the global problem of coral reefs death due to global environmental changes and rising sea water temperatures[10,11], we focused on corals that could be raised and cultivated on land, rather than in the ocean.

Current progress in research and development of scaffold materials has made it possible to regenerate the jawbone defects[12]. In the present study, we processed the exoskeleton of the *montipora digitata* as a bone replacement material and observed it *in vitro* and *in vivo* to obtain basic data on alveolar bone regeneration.

MATERIALS AND METHODS

Processing of coral (montipora digitata) and granule production

We obtained the exoskeleton of a three-year old land-bred edaphic coral (Sea seed, Okinawa, Japan)[6,13]. Corals

Received Sep 26, 2022: Accepted Nov 16, 2022
doi:10.4012/dmj.2022-214 JOI JST.JSTAGE/dmj/2022-214

were composed of polyps, cells, and coral exoskeletons. Polyps comprised soft tissue and exoskeletons included hard tissue. Polyps are thought to be members of the *Anemone* family, and zooxanthellae symbiotic with polyps form the exoskeleton. Polyps were present in the superficial layers of the exoskeleton, ranging from a few to several tens of micrometers in thickness. To remove coral polyps and zooxanthellae attached to the surface layer of the exoskeleton, the specimens were immersed in sodium hypochlorite (6%)[14]. Subsequently, they were rinsed and dried at 70°C for 6 h. Coral granules (CG) of 600–1,000 μm diameter were prepared by grinding in a mortar while using an automatic shaker. Under negative pressure, the granules were immersed in hypochlorous acid (6%) for 24 h, rinsed, dried at 70°C for 6 h, and sterilized with UV light. The prepared CG were used as bone replacement material derived from coral exoskeleton.

Characterization of bone replacement material derived from coral exoskeleton

Diffraction was performed using an X-ray diffractometer (XRD; Lab X XRD-6000, SHIMADZU, Kyoto, Japan). The X-ray source was Cu; the voltage and current were set to 40 kV and 30 mA, respectively. Measurement was performed with CG on a sample table. Elements constituting CG were measured using an X-ray photoelectron spectrometer (XPS; PHI X-tool, ULAVAV-PHI, Kanagawa, Japan). The X-ray source was AlKα, and the output was set to 15 kV and 22 W. The composition of CG was measured using a Fourier transform infrared spectrophotometer (FTIR; IRAffinity-1s, Shimadzu). The internal microstructure of CG was observed using a microfocus X-ray CT (SKYSCAN1275, Bruker, Kanagawa, Japan). The osmium was deposited in vacuum using an osmium coater (HPC-20, VACUUM DEVICE, Ibaraki, Japan), and the surface microstructure of the CG was observed using a scanning electron microscope (SEM; S-4800, Hitachi, Tokyo, Japan).

Cell culture

Human periodontal ligament fibroblast (HPLF; Science Cell Research Laboratories, Carlsbad CA, USA) cell suspension adjusted to a cell density of 2.0×10^5 cells/mL was seeded onto 96-well cell culture plates (Iwaki, Osaka, Japan) at 37°C in a 5% CO_2 atmosphere. After incubation for 1 and 7 days, 3-(4, 5-dimethylthiazolyl-2)-2, 5-diphenyltetrazolium bromide assay was performed using Cell Count Regent SF (NACALAI TESQUE, Kyoto, Japan) and Multi Plate Reader (Spectra Max M50S, MOLECULAR DEVICES, Tokyo, Japan). Mitochondrial activity was measured. The experimental group was defined as that with CG added at the beginning of culturing. The control group was defined as that without adding CG; the amount of CG added was 25 mg/well.

Animal experiments

Four healthy two-year-old female beagle dogs, weighing approximately 10 kg, were used in this experiment. The female beagle dogs were housed at Hamaguchi Lab Plus (Osaka, Japan). The animals received water and pelleted rations *ad libitum* throughout the experiment. The experimental protocol was in accordance with the Regulations for the Use and Care of Animals of Osaka Dental University (approval No. 2205003). Surgical procedures were performed using intravenous, butorphanol (Betorphanol®, Meiji Seika Pharma, Yokohama, Japan), and medetomidine hydrochloride (Domitor®, Nippon Zenyaku Kogyo, Fukushima, Japan) as preanesthetic agents, followed by intravenous pentobarbital sodium (NACALAI TESQUE) as anesthetic induction agent. After confirming sedation, isoflurane (Abbott Japan, Tokyo, Japan) was inhaled as an inhalation anesthetic, the mandible was locally anesthetized with lidocaine (2%) hydrochloride (Aura®, Morita, Osaka, Japan), and bilateral mandibular second premolars and bilateral mandibular fourth premolars were extracted. After eight weeks of healing of the extraction site, the buccal and lingual mucoperiosteal flaps extending from the mandibular first premolar to mandibular first posterior molar were debrided. Thereafter, notches were made at the cemento-enamel junction (CEJ) and the sub-basal portion of the bone defect. A motorized bone surgery instrument (Morita, Kyoto, Japan) was used to create one-wall infrabony defects with a depth of 5 mm and a width of 3 mm in the jawbones. The defects were created in three locations: proximal and distal sides of the mandibular third

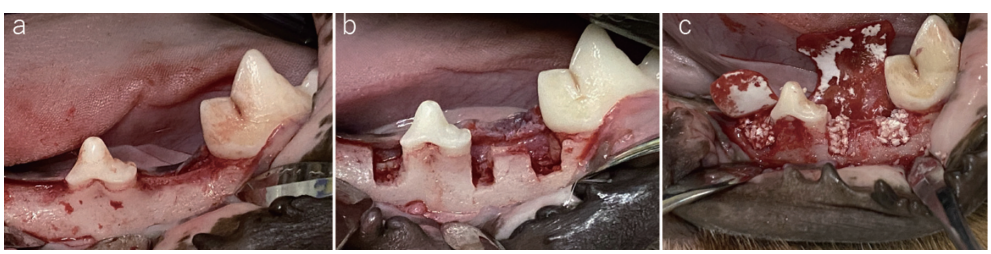

Fig. 1 Gross findings in the experimental group.
a: Gross findings at 8 weeks after tooth extraction. The extraction wound has healed. b: Experimental single-walled bone defect model is created in the proximal and distal third premolar and the proximal first posterior molar. c: Coral exoskeleton-derived bone grafts and placement of an absorbable membrane in the experimental single-walled bone defect model.

premolar and proximal side of the mandibular first posterior molar. The bone defects without CG filling were used as the control group and those with CG filling were used as the experimental group (Fig. 1). An absorbable membrane (GC Membrane, GC, Tokyo, Japan) was then applied and the wound was sutured. For postoperative infection control, an antibacterial drug (pediatric azithromycin®, Pfizer, New York, NY, USA) was orally administered for three days.

Gross findings and radiography

Intraoral photographs were recorded for gross findings immediately after experimental bone defect formation, immediately after placing bone filler, and two months after tooth extraction. Dental radiographs were immediately recorded before tooth extraction, two months after tooth extraction, after experimental bone defect formation, and eight weeks after CG filling. At eight weeks after CG filling, intraoral radiographs of the mandibular premolar area were recorded using an X-irradiator and charge-coupled device sensor.

Microfocus X-ray CT image and histopathology specimen preparation

The control and experimental groups were euthanized by overdosing with sodium pentobarbital (NACALAI TESQUE) eight weeks after CG filling. Following euthanasia, the jawbones were removed and micro-CT imaging was performed, and histopathological specimens were prepared. The mandible was fixed in neutral buffered formalin solution (10%) and then demineralized in ethylenediaminetetraacetic acid (EDTA) solution (10%) for 63 days followed by hematoxylin-eosin (HE) staining and tartrate-resistant anti phosphatase (TRAP) staining. These stained samples were examined under microscope.

The data obtained were analyzed using ystat (Igakutosho Shuppan, Saitama, Japan). The Students' *t*-test was performed. The level of significance was set at $p<0.05$.

RESULTS

Processing and granule production of edaconite coral

The granule size of CG was 600–1,000 μm (Fig. 2). The granule was white in color without odor.

Characterization of bone replacement material derived from coral exoskeleton

XRD revealed the representative patterns of cultured coral particles. Samples with predominantly aragonitic composition showed diffraction peaks of a111, a021, a012, a200, a130, a220, a221, a041, a132, and a113 (Fig. 3). The elements in CG showed XPS peaks with phosphorus peaks (Fig. 4). FTIR spectroscopy provided additional information on the structure of cultured coral particles (Fig. 5). The spectral data of the cultured coral particles revealed strong absorption characteristic peaks at approximately 1,455, 1,082, 852, 709 and 700 cm^{-1}, which have been reported to be the typical mineral of aragonite[15]. Microfocus CT images are shown in Fig. 6. The internal structure of CG was porous, continuous, and permeable with a lumen diameter of approximately 200 μm (Figs. 6a, b). The ducts, 100–200 μm in diameter,

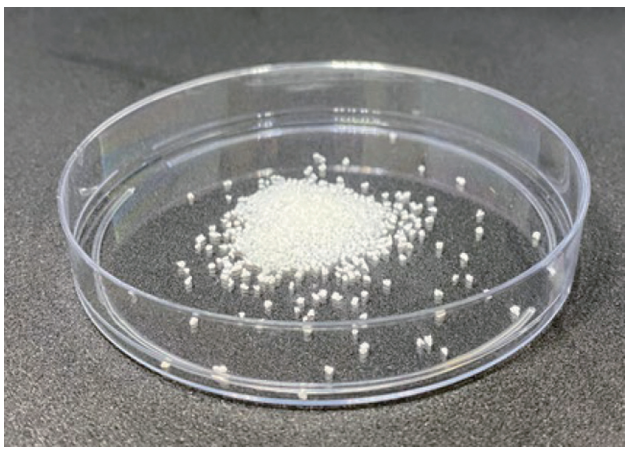

Fig. 2 Processing of coral exoskeleton-derived bone replacement material.

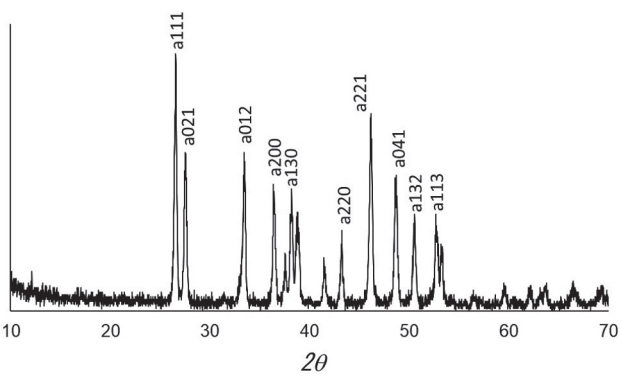

Fig. 3 X-ray diffraction results of coral exoskeleton-derived bone replacement material.

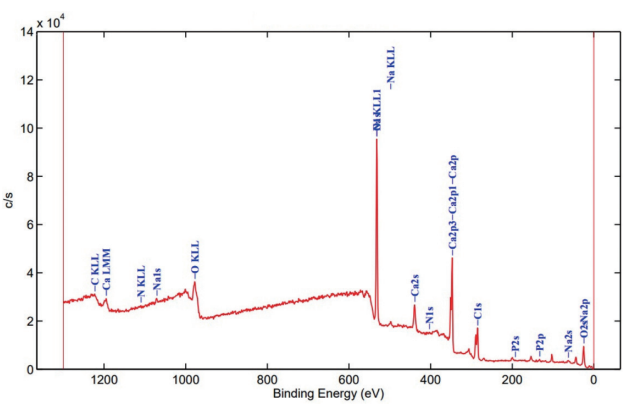

Fig. 4 X-ray photoelectron spectroscopy analysis results of coral exoskeleton-derived bone replacement material.

penetrated to the outside[3]. SEM images are shown in Fig 7. The surface microstructure of CG was coarse (Fig. 7).

Cell culture

Comparing between the non-CG-added (control) and the CG-added (experimental) groups, no significant difference (t-test; $p<0.05$) in mitochondrial activity was observed one day after incubation. Seven days after incubation, mitochondrial activity increased in the experimental group, showing a significant difference between the control and experimental groups ($p<0.05$, Fig. 8).

Animal experiments

Gross observation of the control and experimental groups at eight weeks after creating the experimental unifacial bone defect model showed no change between the two groups: wounds healed in both groups. Radiographic comparison showed horizontal alveolar bone loss in the control group (Fig. 9e). However, no horizontal alveolar bone loss was observed in the experimental group. In addition, more bone growth at the alveolar apex than that in the control group was found (Fig. 10f). The mandible extracted after eight weeks of CG filling was observed by microfocus CT. Compared to the experimental group, the control group showed vertical bone resorption (Fig. 11). According to the HE-stained histopathological images, the alveolar bone near the

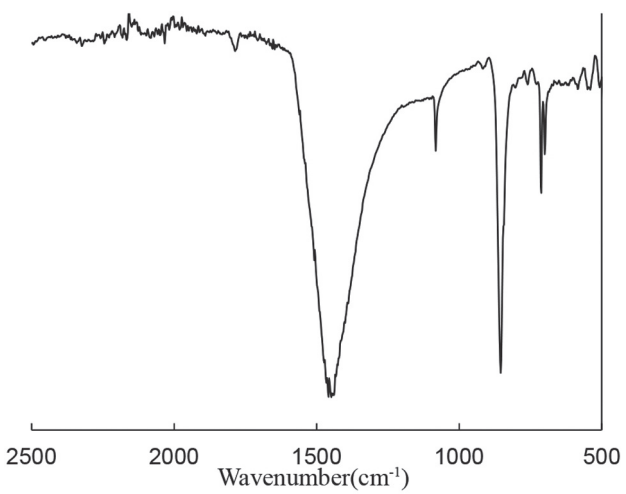

Fig. 5 Fourier transform infrared spectroscopy results of coral exoskeleton-derived bone replacement material.

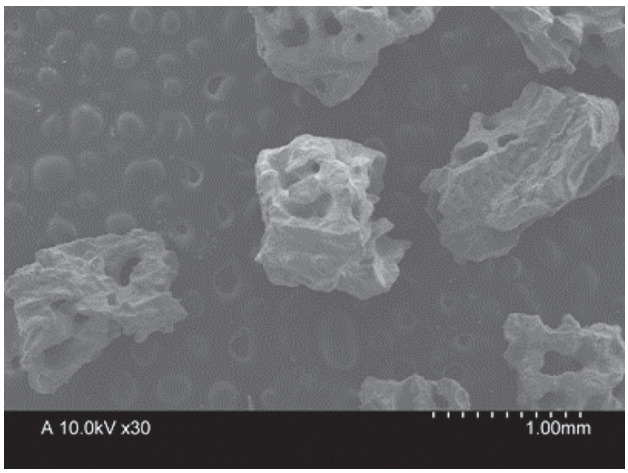

Fig. 7 SEM image of coral exoskeleton-derived bone replacement material.

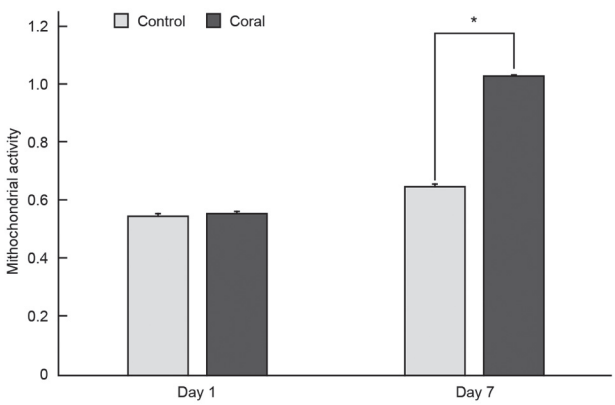

Fig. 8 Comparison of mitochondrial activity.

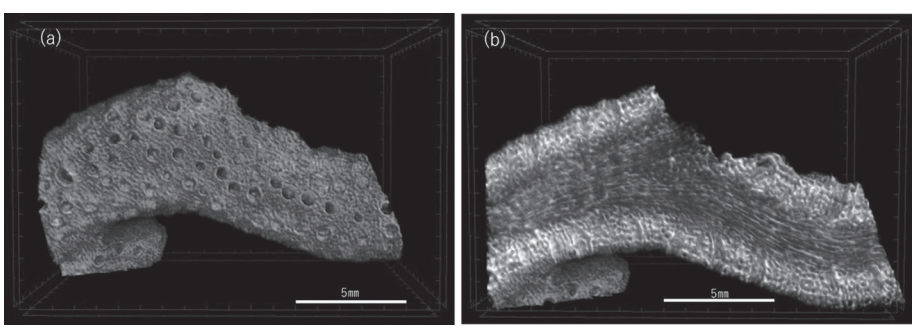

Fig. 6 Microfocus X-ray computed tomography image of coral exoskeleton-derived bone replacement material. a: Coral exoskeleton, b: Cross section of coral exoskeleton

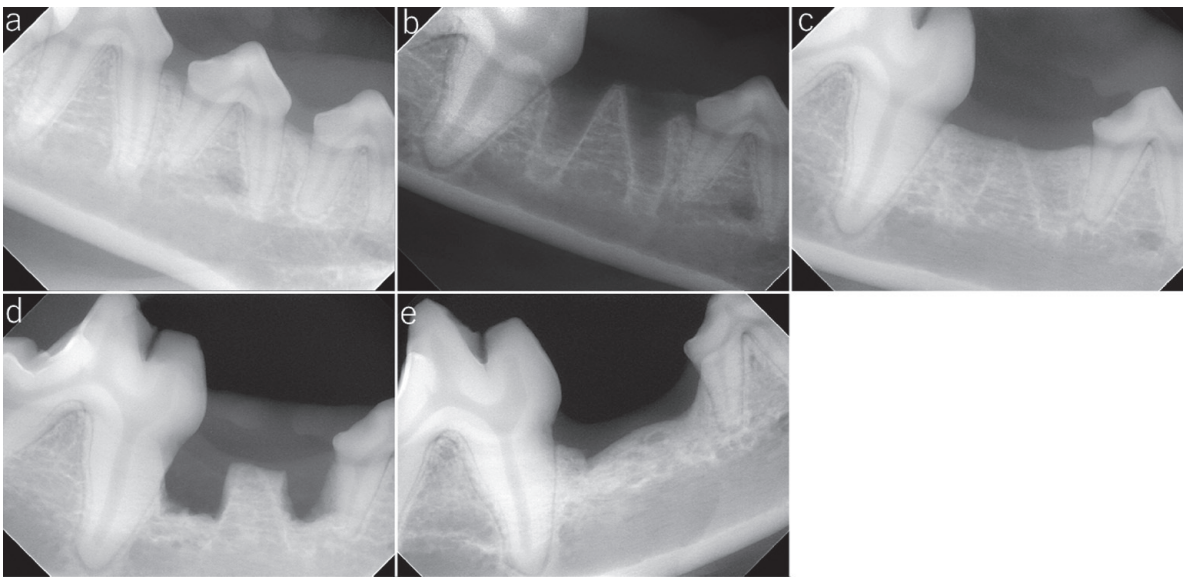

Fig. 9 Radiograph of mandibular right fourth premolar and first posterior molar.
a: Preoperative condition of the mandibular right fourth premolar and mandibular right first posterior molar. b: Immediately after extracting the mandibular right fourth premolar. c: Eight weeks after extraction. d: Immediately after creating a experimental single-walled bone defect model distal to the mandibular right third premolar and proximal to the mandibular right first posterior molar. c: Healing of the extraction wound eight weeks after extraction. d: Immediately after creating the experimental single-walled bone defect model in the centrum of the mandibular right third premolar and at the proximal portion of the mandibular right first posterior molar. e: Eight weeks after creating the experimental single-walled bone defect model. The mandibular right alveolar bone shows bone resorption and partial reduction of the alveolar crest.

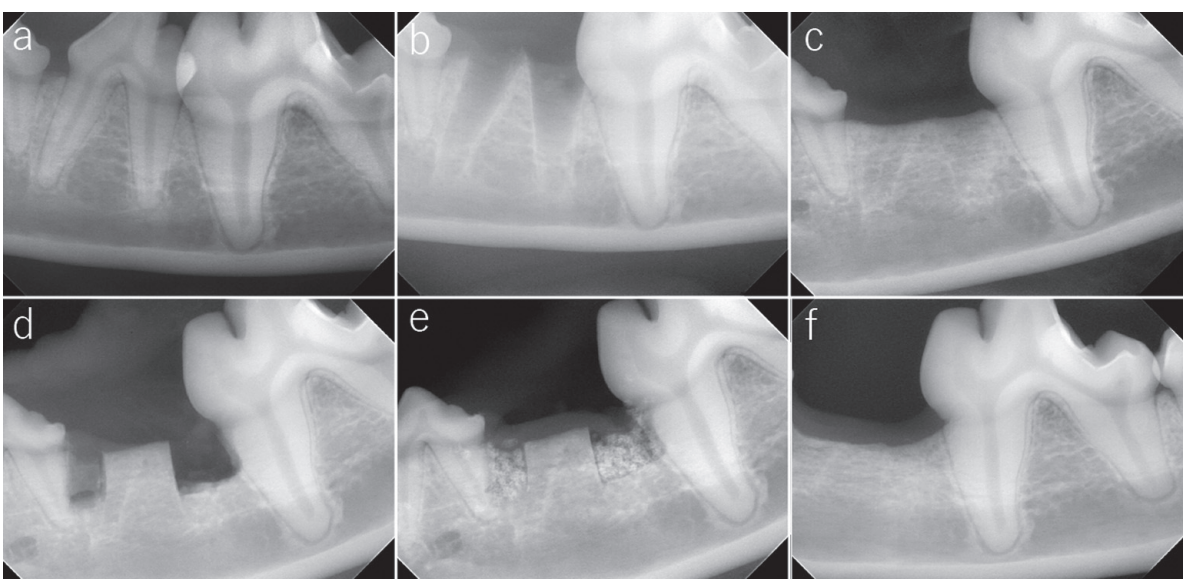

Fig. 10 Radiograph of mandibular left fourth premolar and first posterior molar.
a: Preoperative condition of the mandibular left fourth premolar and mandibular left first posterior molar. b: Immediately after extracting the mandibular left fourth premolar. c: Eight weeks after extraction. d: The centrum of the mandibular left third premolar and mandibular left first posterior molar. d: Immediately after fabricating the experimental single-walled bone defect model of a mandibular left third premolar centrally and a mandibular left first posterior molar proximally. e: Immediately after filling the experimental single-walled bone defect with a coral exoskeleton-derived bone graft. f: Immediately after filling the experimental single-walled bone defect with a coral exoskeleton-derived bone graft. f: Eight weeks after filling with coral exoskeleton-derived bone graft. Compared to that in the control group (Fig. 9e), bone augmentation is seen at the alveolar crest in the experimental group.

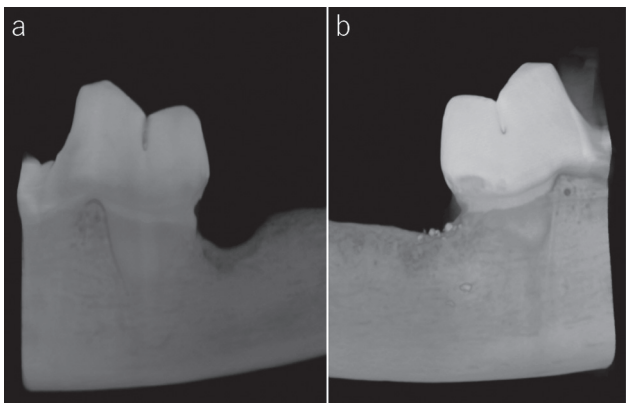

Fig. 11 Three-dimensional image taken by microfocus computed tomography.
a: Eight weeks after non-infusion of coral exoskeleton-derived bone graft. b: Eight weeks after placing the coral exoskeleton-derived bone filler. Impermeability like coral exoskeleton-derived bone filler is observed in the proximal portion of the mandibular left first posterior molar, and bone augmentation of the alveolar crest is observed on comparison with figure a.

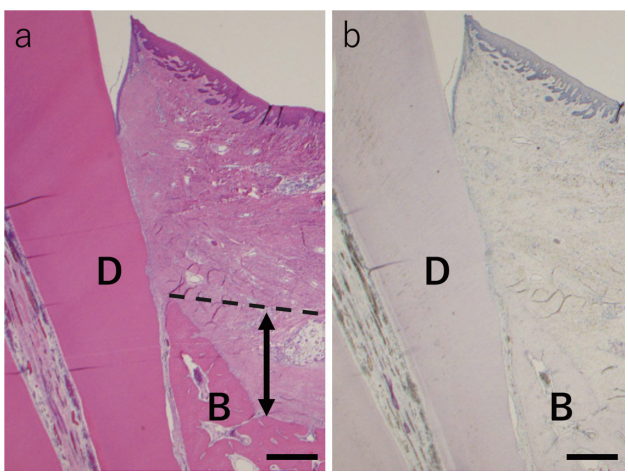

Fig. 12 Histopathology at 8 weeks postoperatively in the control group.
a: Hematoxylin-eosin staining. Alveolar bone resorption is seen (bilateral arrows). b: TRAP staining; no TRAP-positive cells are seen. B, bone; D, dentin. Scale bar indicates 100 µm.

extraction socket in the control group was concave like a plate (Fig. 12a). TRAP staining showed no positive cells in the control group (Fig. 12b). However, positive giant cells were observed around the slightly residual CG in the experimental group (Fig. 13b).

DISCUSSION

Periodontology generally focuses on wound excision of

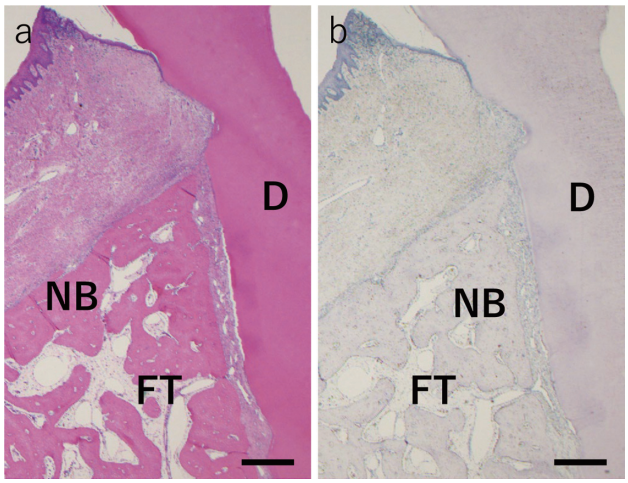

Fig. 13 Histopathology at 8 weeks postoperatively in the experimental group.
a: Hematoxylin-eosin staining. No alveolar bone resorption is seen compared to the control group (Fig. 11a). b: TRAP staining with a few TRAP-positive cells. NB, new bone; D, dentin; FT, fatty marrow. Scale bar indicates 100 µm.

periodontal pockets. Moreover, in the past, artificial scaffold materials were not used for treatment[16,17]. However, materials have now been developed for periodontal tissue regeneration after periodontal disease[18-21]. Most of the ready-made coral exoskeleton-derived bone replacement materials commercially available in Europe and the United States are made from Scleractinia and *Goniopora*[22,23]. *Montipora digitata* can be cultured on land and produced as a closed colony[24], which is considered desirable as a raw material for synthesizing medical devices from the perspective of sustainable development goals (SDGs)[25] and stable supply. SEM observation showed that the surface of CG with a diameter of 600–1,000 µm had a coarse and porous structure similar to that of Cerasolve® (ZimVie, Tokyo, Japan). *Montipora digitata* is known to be easily absorbed by living organisms due to its physical and chemical properties[25]. The characteristic difference between Scleractinia, *Goniopora* and *Montipora distata* as bone replacement material lies in their porosity. The porosity of *Montipora digitata* is known to be higher than that of Scleractinia and *Goniopora*[7,26].

In this study, coral-derived phosphorus peaks were detected by XPS. Although previous CG XRD studies have detected the aragonite crystalline phase[27], no peaks associated with the calcite phase were observed[15,28]. FTIR spectroscopy results have shown strong absorption bands associated with the typical mineral of aragonite. The FTIR peak at approximately 1,082 cm^{-1} was observed only in the spectrum of calcium carbonate of the aragonite phase, whose CO_3^{2-} ions were inactive in the infrared region[29]. Calcium carbonate bone replacement materials derived from natural coral exoskeleton (aragonite) were resorbed and reconstructed more quickly than

were calcium phosphate bone replacement materials[30]. Similar to coral exoskeleton-derived bone replacement materials commercially available in Europe and the United States, CG may promote bone regeneration in the alveolar and periapical bone.

The exoskeleton of planktonic corals is composed of calcite, a crystal of calcium carbonate, and is known to have sufficient physical strength[20]. In general, the finer a material is, the more its compressive strength tends to increase[8,26,31]. In addition, the oral cavity is an environment where gingival and periodontal tissues are subjected to physical stimuli during chewing and swallowing. It is a harsh environment for procedures that target bone tissue regeneration. In the present experiment, a sufficient amount of alveolar bone growth was observed in the experimental group in one-wall infrabony defects. In addition, the 600–1,000 μm diameter of CG was maintained after placement in the defect until it was replaced by bone tissue. The experimentally created one-wall infrabony defect was found to be incapable of self-healing in the control group. The created jawbone defects could not be self-healed in the experimental group. Therefore, CG with a prototype diameter of 600–1,000 μm was applied as a bone replacement material to the defect for regenerating bone tissue and maintaining the anatomical morphology before bone loss. Despite physical stimulation from chewing and swallowing for 8 weeks, CG was replaced by bone tissue. This suggests that CG has the physical properties required as a bone replacement material for jawbone regeneration despite its fine-structured granules.

Montipora digitata exoskeleton-derived bone regenerator is known to show advantageous ability as a bone regenerator when co-cultured with some cells[26,32,33]. CG with a granule diameter of 600–1,000 μm used in this study significantly enhanced mitochondrial activity in co-culture with human fibroblasts. These results are consistent with the possibility that calcium carbonate derived from coral exoskeletons promotes mitochondrial activity, cell proliferation, and collagen fiber production in co-culture with human fibroblasts, favoring granulation tissue formation for tissue defect repair and regeneration.

Radiographs and histopathology with H-E staining showed that self-healing could not be achieved in the control group and large bone defects remained. On the other hand, the experimental group showed regeneration of the alveolar bone, alveolar hard line, periodontal ligament space, and periodontal ligament at 8 weeks postoperatively, despite creating an experimental bone defect that could not self-heal. This means that CG may enable regeneration of not only alveolar bone, but also periodontal ligament when applied as a bone replacement material to unifacial bone defects that cannot heal on their own. Although exoskeleton-derived bone filler of *Montipora digitata* in block form is bioabsorbable[23], the bioabsorbability of CG with a granule diameter of 600–1,000 μm in the jawbone has been unknown to date. TRAP-stained pathology at 8 weeks postoperatively in the experimental group showed that most of the CG was lost or absorbed, and TRAP-positive giant cells were observed on the outer surface and around the luminal structures of the few remaining CGs. These results indicate that CG might have the ability to be almost completely absorbed by the body in a short period of time (8 weeks) in large bone defects. Based on these findings, it is possible that CG is completely bioabsorbable. This could be expected to result in earlier recovery compared to that provided by the existing products used for repairing similar bone defects[34]. When porous hydroxyapatite and exoskeleton-derived granules of *Montipora digitata,* as bone replacement material, were applied to extraction sockets, it was found that coral granules could be resorbed earlier at 12 weeks after surgery.

In conclusion, CG used in this experiment was porous, having continuous scaffold material bioabsorbable properties, and could be rapidly resorbed, while maintaining its filled shape. This suggested that CG may be useful for regeneration of alveolar and jaw bone with large defects. CG is expected to enable early regeneration of bone defects that cannot heal on their own due to its physical and chemical properties. On the other hand, the CG used in this study was only a prototype. However, to develop it as a medical device, it might be necessary to verify its efficacy for other applications required in clinical dentistry in terms of performance and manufacturing. Moreover, it is necessary to review its manufacturing, sterilization, and storage methods. Accelerated degradation tests should also be performed to verify quality stability of CG, and the final product specifications need to be established.

ACKNOWLEDGMENTS

The authors acknowledge the assistance of Naoya Uemura (Department of Oral Implantology, Osaka Dental University) with the animal experiments. This work was supported by JSPS KAKENHI Grant Number JP21K17016.

REFERENCES

1) Darby I. Periodontal materials. Aust Dent J 2011; 56: 107-118.
2) Peppas NA, Langer R. New challenges in biomaterials. Science 1994; 263: 1715-1720.
3) Nishikawa T, Okamura T, Kokubu M, Kato H, Imai K, Ono T, *et al.* Morphological and physical characteristics and cell affinity of coral as a scaffold. J Oral Tissue Engin 2011; 9: 88-95.
4) Nishikawa T, Okamura T, Masuno K, Matsumoto H, Hirose M, Uemura N, *et al.* Comparative study of physical and morphological characteristics of cultured and natural coral as a bone augmentation scaffold. J Oral Tissue Engin 2016; 14: 107-113.
5) Nishikawa T, Okamura T, Ono T, Matsushita H, Imai K, Honda Y, *et al.* Bone augmentation experiment using coral on the skull of rat. Nano Biomed 2013; 5: 109-113.
6) Matuda Y, Nishikawa T, Okamura T, Kazuya T, Wato M, Tabata H, *et al.* Comparative study of tissue affinity, chemical characteristics of cultured and natural coral as a bioabsorbable scaffold. J Oral Tissue Engin 2017; 14: 164-

170.
7) Nishikawa T, Okamura T, Masuno K, Tominaga K, Wato M, Kokubu M, *et al.* Physical characteristics and interior structure of coral skeleton as a bone scaffold material. J Oral Tissue Engin 2009; 7: 121-127.
8) Wu Y-C, Lee T-M, Chiu K-H, Shaw S-Y, Yang C-Y. A comparative study of the physical and mechanical properties of three natural corals based on the criteria for bone–tissue engineering scaffolds. J Mater Sci Mater Med 2009; 20: 1273-1280.
9) Fricain JC, Roudier M, Rouais F, Basse-Cathalinat B, Dupuy B. Influence of the structure of three corals on their resorption kinetics. J Periodontal Res 1996; 31: 463-469.
10) Anthony KR, Marshall PA, Abdulla A, Beeden R, Bergh C, Black R, *et al.* Operationalizing resilience for adaptive coral reef management under global environmental change. Glob Chang Biol 2015; 21: 48-61.
11) Hoegh-Guldberg O, Mumby PJ, Hooten AJ, Steneck RS, Greenfield P, Gomez E, *et al.* Coral reefs under rapid climate change and ocean acidification. Science 2007; 318: 1737-1742.
12) Palti A, Hoch T. A concept for the treatment of various dental bone defects. Implant Dent 2002; 11; 73-78.
13) Satoh N, Kinjo K, Shintaku K, Kezuka D, Ishimori H, Yokokura A, *et al.* Color morphs of the coral, Acropora tenuis, show different responses to environmental stress and different expression profiles of fluorescent-protein genes. G3 2021; 11: jkab018.
14) Luo Y, Zhao J, He C, Lu Z, Lu X. Miniaturized platform for individual coral polyps culture and monitoring. Micromachines 2020; 11: 127.
15) Mansur HS, Mansur AA, Pereira M, editors. XRD, SEM/EDX and FTIR characterization of Brazilian natural coral. Key Engin Mater 2005: 284: 43-46.
16) Phillips RW. Report of the committee on scientific investigation of the american academy of restorative dentistry. J Prosthet Dent 1990; 64: 74-110.
17) Ramfjord SP. Design of studies or clinical trials to evalute the effectiveness of agents or procedures for the prevention, or treatment, of loss of the periodontium. J Periodontal Res 1974; 9: 78-88.
18) Hieda A, Uemura N, Hashimoto Y, Toda I, Baba S. In vivo bioactivity of porous polyetheretherketone with a foamed surface. Dent Mater J 2017; 36: 222-229.
19) Matsuse K, Hashimoto Y, Kakinoki S, Yamaoka T, Morita S. Periodontal regeneration induced by porous alpha-tricalcium phosphate with immobilized basic fibroblast growth factor in a canine model of 2-wall periodontal defects. Med Mol Morphol 2018; 51: 48-56.
20) Matuda Y, Okamura T, Tabata H, Yasui K, Tatsumura M, Kobayashi N, *et al.* Periodontal regeneration using cultured coral scaffolds in class ii furcation defects in dogs. J Hard Tissue Biol 2019; 28: 329-334.
21) Zhao J, Honda Y, Tanaka T, Hashimoto Y, Matsumoto N. Releasing behavior of lipopolysaccharide from gelatin modulates inflammation, cellular senescence, and bone formation in critical-sized bone defects in rat calvaria. Materials (Basel) 2020; 13: 95.
22) Green DW, Ben-Nissan B, Yoon KS, Milthorpe B, Jung HS. Natural and synthetic coral biomineralization for human bone revitalization. Trends Biotechnol 2017; 35: 43-54.
23) White RA, Weber JN, White EW. Replamineform: A new process for preparing porous ceramic, metal, and polymer prosthetic materials. Science 1972; 176: 922-924.
24) Abrego D, Willis BL, van Oppen MJ. Impact of light and temperature on the uptake of algal symbionts by coral juveniles. PLoS One 2012; 7: e50311.
25) Kawamura K, Nishitsuji K, Shoguchi E, Fujiwara S, Satoh N. Establishing sustainable cell lines of a coral, Acropora tenuis. Mar Biotechnol 2021; 23: 373-388.
26) Okamura T, Uemura N, Baba S, Yasuda N, Yamashiro H, Imai K, *et al.* Montipora digitata exoskeleton derived aragonite particles are useful scaffold for tissue-engineered vascular graft in vitro. Nano Biomed 2017; 9: 105-111.
27) Kontoyannis CG, Vagenas NV. Calcium carbonate phase analysis using XRD and FT-Raman spectroscopy. Analyst 2000; 125: 251-255.
28) Sivakumar M, Sampath Kumar TS, Shantha KL, Panduranga Rao K. Development of hydroxyapatite derived from Indian coral. Biomaterials 1996; 17: 1709-1714.
29) Shafiu Kamba A, Ismail M, Tengku Ibrahim TA, Zakaria ZAB. Synthesis and characterisation of calcium carbonate aragonite nanocrystals from cockle shell powder (Anadara granosa). J Nanomater 2013; 2013: 398357.
30) Umemoto S, Furusawa T, Unuma H, Tajika M, Sekino T. In vivo bioresorbability and bone formation ability of sintered highly pure calcium carbonate granules. Dent Mater J 2021; 40: 1202-1207.
31) Holmes RE, Bucholz R, Mooney V. Porous hydroxyapatite as a bone-graft substitute in metaphyseal defects. A histometric study. J Bone Joint Surg Am 1986; 68: 904-911.
32) Okamura T, Nishikawa T, Wato M, Tominaga K, Kato H, Imai K, *et al.* Application of porous materials to three-dimensional tissue culture in capillary formation in vitro. J Oral Tissue Engin 2014; 12: 93-99.
33) Okamura T, Takeuchi T, Honda S, Tominaga K, Naruse K, Morita S, *et al.* Effects of Montipora digitata exoskeleton-derived aragonite particles on human fibroblasts for cell proliferation and collagen production in vitro. J Oral Tissue Engin 2017; 15: 41-48.
34) Ono T, Nishikawa T, Tanaka A, Matsumoto N. Histological reaction to porous coral and ceramic bone. J Oral Tissue Engin 2013; 11: 85-97.